bioRxiv preprint doi: https://doi.org/10.1101/589465; this version posted March 29, 2019. The copyright holder for this preprint (which was not certified by peer review) is the author/funder, who has granted bioRxiv a license to display the preprint in perpetuity. It is made available under aCC-BY-NC-ND 4.0 International license.

Seasonal stability and dynamics of DNA methylation in plants in a natural environment

Tasuku Ito[a], Haruki Nishio[a], Yoshiaki Tarutani[b], Naoko Emura[a,c], Mie N. Honjo[a], Atsushi Toyoda[d,e], Asao Fujiyama[e], Tetsuji Kakutani[b,f], and Hiroshi Kudoh[a,1].

[a]Center for Ecological Research, Kyoto University, Otsu, Shiga 520–2113, Japan; [b]Department of Chromosome Science, National Institute of Genetics, Mishima, Shizuoka 411-8540, Japan; [c]Faculty of Agriculture, Kagoshima University, Korimoto 1-21-24, Kagoshima 890-0065, Japan; [d]Department of Genomics and Evolutionary Biology, National Institute of Genetics, Mishima, Shizuoka 411-8540, Japan; [e]Advanced Genomics Center, National Institute of Genetics, Mishima, Shizuoka 411-8540, Japan; [f]Department of Biological Sciences, Graduate School of Science, The University of Tokyo, Hongo, Bunkyo-ku, Tokyo 113-0033, Japan

bioRxiv preprint doi: https://doi.org/10.1101/589465; this version posted March 29, 2019. The copyright holder for this preprint (which was not certified by peer review) is the author/funder, who has granted bioRxiv a license to display the preprint in perpetuity. It is made available under aCC-BY-NC-ND 4.0 International license.

[1]Corresponding author: Hiroshi Kudoh; Center for Ecological Research, Kyoto University, Hirano 2-509-3, Otsu, Shiga 520–2113, Japan; Phone, +81-77-549-8205; E-mail, kudoh@ecology.kyoto-u.ac.jp.

bioRxiv preprint doi: https://doi.org/10.1101/589465; this version posted March 29, 2019. The copyright holder for this preprint (which was not certified by peer review) is the author/funder, who has granted bioRxiv a license to display the preprint in perpetuity. It is made available under aCC-BY-NC-ND 4.0 International license.

Abstract

Organisms survive in naturally fluctuating environments by responding to long-term signals, such as seasonality, by filtering out short-term noise. DNA methylation has been considered a stable epigenetic mark but has also been reported to change in response to experimental manipulations of biotic and abiotic factors. However, it is unclear how they behave in natural environments. Here, we analyzed seasonal patterns of genome-wide DNA methylation at a single-base resolution using a single clone from a natural population of the perennial *Arabidopsis halleri*. The genome-wide pattern of DNA methylation was primarily stable, and most of the repetitive regions were methylated across the year. Although the proportion was small, we detected seasonally methylated cytosines (SeMCs) in the genome. SeMCs in the different contexts showed distinct seasonal patterns of methylation. SeMCs in CHH context were detected predominantly at repetitive sequences in intergenic regions. Additionally, we found that CHH methylation within *AhgFLC* locus showed a seasonal pattern that was negatively associated with changes in gene expression. Gene-body CG

bioRxiv preprint doi: https://doi.org/10.1101/589465; this version posted March 29, 2019. The copyright holder for this preprint (which was not certified by peer review) is the author/funder, who has granted bioRxiv a license to display the preprint in perpetuity. It is made available under aCC-BY-NC-ND 4.0 International license.

methylation (gbM) itself was generally stable across seasons, but the levels of gbM were positively associated with seasonal stability of RNA expression of the genes. These results suggest the existence of two distinct aspects of DNA methylation in natural environments: sources of epigenetic variation and epigenetic marks for stable gene expression.

Keywords: *Arabidopsis halleri*, DNA methylation, Natural environment, seasonal changes, seasonally methylated cytosines

bioRxiv preprint doi: https://doi.org/10.1101/589465; this version posted March 29, 2019. The copyright holder for this preprint (which was not certified by peer review) is the author/funder, who has granted bioRxiv a license to display the preprint in perpetuity. It is made available under aCC-BY-NC-ND 4.0 International license.

Introduction

DNA methylation at cytosine residues is an epigenetic mark that can be maintained through cell divisions in a wide range of eukaryotic genomes (1).The previous analyses in diverse organisms have revealed genomic distributions of DNA methylation vary among organisms (2-7). In plants, DNA-methylation varies both between and within species (8), and sometimes is associated to phenotypic variation (9-11). Although the level and patterns of DNA methylation are heritable to a certain extent, the mechanisms that produce and maintain epigenetic variation across generations are largely unknown.

DNA methylation can vary between individuals also by non-genetic causes. It has been shown that both biotic and abiotic treatment can modify DNA methylation (12-14). Because of its semi-stable and semi-labile nature, non-genetic changes in DNA methylation are not explained by simple environmental effects. For example, even in a genetically homogeneous background under stable laboratory conditions, epigenetic variation in DNA methylation can occur during repeated self-pollination in a transgenerational

bioRxiv preprint doi: https://doi.org/10.1101/589465; this version posted March 29, 2019. The copyright holder for this preprint (which was not certified by peer review) is the author/funder, who has granted bioRxiv a license to display the preprint in perpetuity. It is made available under aCC-BY-NC-ND 4.0 International license.

59 manner (15, 16). Therefore, it is difficult to predict whether DNA methylation is
60 stable or dynamic under natural conditions. Recently the need for '*in natura*'
61 studies has been highlighted in order to understand how organisms respond to
62 environmental signals by filtering out innumerable fluctuations and noise (17, 18).
63 In the temperate regions, seasonality is the most prominent cause of
64 environment fluctuations. However, we still do not understand how DNA
65 methylation behaves across seasons.

66 In order to reveal the seasonal dynamics of DNA methylation, here, we
67 conducted an "*in natura*" study on genome-wide DNA methylation using a single
68 clone growing in a population of *Arabidopsis halleri* (L.) O'Kane & Al-Shehbaz
69 subsp. *gemmifera* (Matsum.) O'Kane & Al-Shehbaz (hereafter referred to as *A.*
70 *haleri*), a close relative of *Arabidopsis thaliana*. Its clonal propagation and
71 perennial life-cycle allowed us to sample leaves all year round from the single
72 clonal individual (19). We studied seasonal dynamics of key flowering-time
73 genes and whole transcriptome previously in the site (20, 21). In this study, to
74 understand the dynamics of DNA methylation, we performed whole-genome

bioRxiv preprint doi: https://doi.org/10.1101/589465; this version posted March 29, 2019. The copyright holder for this preprint (which was not certified by peer review) is the author/funder, who has granted bioRxiv a license to display the preprint in perpetuity. It is made available under aCC-BY-NC-ND 4.0 International license.

bisulfite sequencing (WGBS) at 1.5-month intervals, over a year, under natural conditions. We adopted the strategy of monitoring the seasonal pattern in a single clonal individual with a uniform genetic background.

DNA methylation occurs in three contexts, according to the flanking sequence, i.e. CG, CHG and CHH (H = A, C, or T). The former two form symmetrically and the latter one asymmetrically, in terms of sequences on the complementary strands. Since these contexts of methylation are distinctly regulated and associated with DNA replication, histone modification, and non-coding RNA production (22-24), we examined seasonal patterns of DNA methylation by conducting single-base resolution analyses.

The results suggested the existence of seasonally methylated cytosines (SeMCs) in the genome, at least for the examined clone. Interestingly, DNA methylation changes occurred in a context-dependent manner. There were distinct patterns of seasonal changes among CG, CHG, and CHH methylation. Moreover, our analysis revealed that genic CG methylation, i.e. gene-body methylation (gbM), was seasonally stable by itself, and was associated with

bioRxiv preprint doi: https://doi.org/10.1101/589465; this version posted March 29, 2019. The copyright holder for this preprint (which was not certified by peer review) is the author/funder, who has granted bioRxiv a license to display the preprint in perpetuity. It is made available under aCC-BY-NC-ND 4.0 International license.

seasonal stability of RNA expression. This study suggested not only that there is a dynamic nature in DNA methylation in plants in their natural habitats, but also highlights the implications of DNA methylation in robust maintenance of stable RNA expression.

Results

Seasonal stability in large-scale distribution of DNA methylation. To investigate the dynamics of DNA methylation in a natural environment, we analyzed genome-wide DNA methylation in a natural population of *A. halleri* (Fig. 1 *A* and *B*). In the study site, the hourly air temperature ranged from -4.3 °C to 36.3 °C during the one-year study period, from Nov 2014 to Sep 2015 (Fig. 1*C*). We collected leaves from a single clonal patch of *A. halleri* at 8 sampling times, at 1.5-month intervals across a year, and performed WGBS (Fig. 1*C*). From this, we obtained a series of genome-wide DNA methylation data (Table S1).

Bulk DNA methylation levels were relatively constant across the eight time points, and ca 45%, 20%, and 6% of cytosines in the genome were kept

bioRxiv preprint doi: https://doi.org/10.1101/589465; this version posted March 29, 2019. The copyright holder for this preprint (which was not certified by peer review) is the author/funder, who has granted bioRxiv a license to display the preprint in perpetuity. It is made available under aCC-BY-NC-ND 4.0 International license.

methylated in CG, CHG, and CHH contexts, respectively (Fig. S1*A*). The large-scale distribution of DNA methylation was determined by the positions in the genome, as represented by radial patterns in the circos plot for the longest 30 scaffolds (Fig. 2*A*). The distribution of methylated sites remained constant across the 8 sampling times (represented by 8 concentric circles for each methylation context in Fig 2*A*). We observed conspicuous aggregation of DNA methylation on repetitive sequences (Fig 2*A*). For example, scaffolds 3 and 18 is characterized by low and high density of repetitive sequences that corresponded to relatively low and high methylation levels, respectively (Fig 2*A*). In the comparative analysis between genic and repetitive regions for the whole genome, the level of DNA methylation in repetitive sequences was higher than that in genes (Fig. S1*B*). A similar pattern was confirmed by an analysis using 100 kbp windows for the whole genome (Fig. 2*B*). The level of DNA methylation was correlated with density of repeats in each window for all three contexts in all samples (e.g. Fig. 2*B* for Nov. 2014, Pearson's correlation coefficients were 0.64, 0.68, and 0.70 for CG, CHG, and CHH context, respectively; Table S2 for the

bioRxiv preprint doi: https://doi.org/10.1101/589465; this version posted March 29, 2019. The copyright holder for this preprint (which was not certified by peer review) is the author/funder, who has granted bioRxiv a license to display the preprint in perpetuity. It is made available under aCC-BY-NC-ND 4.0 International license.

other sampling times). Although aggregation of DNA methylation at repetitive sequences was similar to the patterns previously reported in related Brassicaceae (2, 3, 25), seasonal stability in large-scale distribution of DNA methylation was reported for the first time here.

SeMCs: Seasonal dynamics of DNA methylation. Next, we searched for SeMCs by detecting differently methylated cytosines in the genome across the eight time points (Fisher's exact test; $P < 0.001$; FDR < 0.2). The majority of cytosines did not show statistical differences in methylation across the year, and the proportion of SeMCs was less than 0.5% of total cytosines (Fig. S2 *A* and *B*). Still, we detected 62,716, 47,140, and 179,385 SeMCs in CG, CHG, and CHH contexts, respectively (Fig. 3*A*). They showed diverse seasonal patterns in their level of methylation across the year (Fig. 3*A*). Interestingly, each context of DNA methylation showed distinct patterns of seasonal change: the number of SeMCs that peaked in a particular month was the highest in July, March, and September in CG, CHG, and CHH contexts, respectively (Fig. 3B). Differences among

bioRxiv preprint doi: https://doi.org/10.1101/589465; this version posted March 29, 2019. The copyright holder for this preprint (which was not certified by peer review) is the author/funder, who has granted bioRxiv a license to display the preprint in perpetuity. It is made available under aCC-BY-NC-ND 4.0 International license.

139 contexts of SeMCs would reflect the responsiveness of the regulatory
140 mechanisms of DNA methylation to environmental cues.
141
142 **CHH SeMCs in repetitive sequences**. The distribution of SeMCs in the
143 genome differed between the contexts of DNA methylation. The majority of
144 SeMCs in CHH context (CHH-SeMCs) were found in intergenic regions (those
145 annotated as neither exons nor introns) while CG-SeMCs and CHG-SeMCs
146 were in both genic and intergenic regions (Fig. 4A). Given that large fractions of
147 the eukaryotic genome are intergenic regions and consist of repetitive
148 sequences such as transposable elements (26, 27), we compared the level of
149 CHH methylation for all repetitive sequences in the genome of *A. halleri*. The
150 median level of methylation was the highest in autumn, i.e., September and
151 November (Fig. 4*B*), and the pattern was similar to that of whole-genome
152 CHH-SeMCs. An example of seasonal changes in CHH methylation level in a
153 LINE/L1 showed low and high levels in February-March and
154 September-November, respectively (Fig. 4*C*). The highest methylation levels in

bioRxiv preprint doi: https://doi.org/10.1101/589465; this version posted March 29, 2019. The copyright holder for this preprint (which was not certified by peer review) is the author/funder, who has granted bioRxiv a license to display the preprint in perpetuity. It is made available under aCC-BY-NC-ND 4.0 International license.

155 autumn were detected in other selected families of repetitive sequences, such as
156 LTR/Copia, LTR/Gypsy, LINE/L1, DNA/MULE-MuDR, DNA/hAT, and
157 RC/Helitron (Fig. S3).

158 In addition, we found some repetitive sequences that showed a unique
159 seasonal pattern of CHH methylation. For example, in the intronic repeat at the
160 locus of *FLOWERING LOCUS C* homolog (*AhgFLC*). *AhgFLC* expression is
161 regulated seasonally and suppresses flowering when it is upregulated (20). We
162 found that a SINE-like repetitive sequence in the first intron of *AhgFLC* showed a
163 seasonal change of CHH methylation. The level was the highest in March and
164 the lowest in June (Fig. 4*D*). Interestingly, this seasonal pattern was opposite to
165 that of RNA expression of *AhgFLC* (Fig. 4*E*). The presence of interactions
166 between transcription and CHH methylation in the intragenic repeat at *AhgFLC*
167 is expected.

168

169 **Gene-body CG methylation (gbM) and constant RNA expression.** Previous
170 studies have reported that gbM is localized to active genes in a wide range of

bioRxiv preprint doi: https://doi.org/10.1101/589465; this version posted March 29, 2019. The copyright holder for this preprint (which was not certified by peer review) is the author/funder, who has granted bioRxiv a license to display the preprint in perpetuity. It is made available under aCC-BY-NC-ND 4.0 International license.

171 eukaryotes (5, 6). In *A. thaliana*, DNA methylation at the gene body is primarily
172 observed in CG context (2, 3, 25). We examined seasonal patterns of gbM in *A.*
173 *halleri* and found that the level of gbM was constant across seasons, both in
174 medians and quantiles of all genes (Fig. S4*A*), and at the individual gene level
175 (Fig. S4*B*).

176 In order to examine the potential role of gbM in gene regulation, we tested
177 whether the level of gbM associated to seasonal patterns of RNA expression
178 using previously published data of a two-year seasonal RNA-seq of *A. hallei* at
179 the same study site (21). We found that genes with high gbM often have
180 constant levels of RNA expression across the year. One such example was
181 *AhgPP2AA3* (Fig 5 *A* and *B*), the homolog of *PROTEIN PHOSPHATASE 2A*
182 *SUBUNIT A3*, a gene that is known as one that is constantly-expressed under
183 various conditions in *A. thaliana* (28). This is in contrast to the situation of
184 *AhgFLC* locus, a representative of seasonally expressed genes, which lacks CG
185 methylation from the entire locus, except for the repetitive sequence in the first
186 intron (Fig. 5 *C* and *D*). Based on these observations, we hypothesized that gbM

bioRxiv preprint doi: https://doi.org/10.1101/589465; this version posted March 29, 2019. The copyright holder for this preprint (which was not certified by peer review) is the author/funder, who has granted bioRxiv a license to display the preprint in perpetuity. It is made available under aCC-BY-NC-ND 4.0 International license.

187 would be associated to constant RNA expression across seasons. To test this
188 hypothesis, we calculated the seasonal average and range of RNA expression
189 for each gene, then compared them between genes with different levels of gbM
190 (Fig. 5 *E* and *F*). Genes that were highly methylated in CG context showed
191 relatively high average levels of RNA expression (Fig. 5*E*). The magnitude of
192 seasonal changes in RNA expression of these genes decreased with increasing
193 levels of gbM (Fig 5*F*). These results are consistent with the hypothesis
194 mentioned above. The genes with the highest methylation level (in 'group 5' in
195 Fig 5 *E* and *F*) were weakly enriched with four GOs of basic functions (Table S3).
196

197 **Discussion**

198 In this study, we examined the seasonal patterns of DNA methylation at CG,
199 CHG, and CHH contexts in *Arabidopsis halleri,* under natural conditions. We
200 identified the genomic sites that showed seasonal changes in DNA methylation.
201 Our observations suggest that seasonal factors in the natural habitat could affect
202 DNA methylation differently according to its context and location in the genome.

bioRxiv preprint doi: https://doi.org/10.1101/589465; this version posted March 29, 2019. The copyright holder for this preprint (which was not certified by peer review) is the author/funder, who has granted bioRxiv a license to display the preprint in perpetuity. It is made available under aCC-BY-NC-ND 4.0 International license.

We would like to note here that, since our data set came from a single clonal individual for a single year, the genetic and non-genetic effects between different clones should be explored in future studies by applying WGBS to a population-level study with multiple repeat samples.

CHH methylation showed seasonal changes in diverse repetitive elements, and the level of DNA methylation was high in autumn, and low in winter. In *A. thaliana*, it has been reported that the level of CHH methylation in transposable elements was higher in 16˚C environments relative to 10˚C (13). Additionally, it has been suggested that RNA-directed DNA methylation (RdDM) pathway, which is required for maintenance and *de novo* methylation and mainly targets transposable elements, are involved in heat tolerance (29). This suggests that our observation on CHH SeMCs could reflect the temperature-dependence of the regulation of CHH methylation.

Seasonal changes detected in CHH methylation at a repetitive element in *AhgFLC* was an interesting example showing how genic heterochromatin behaves in genes. We observed that the seasonal pattern of CHH methylation in

bioRxiv preprint doi: https://doi.org/10.1101/589465; this version posted March 29, 2019. The copyright holder for this preprint (which was not certified by peer review) is the author/funder, who has granted bioRxiv a license to display the preprint in perpetuity. It is made available under aCC-BY-NC-ND 4.0 International license.

this particular repetitive element was opposite to that of the expression of *AhgFLC* gene. *FLC* and its homologs in Brassicaceae species contain conserved structures in its second intron called VRE (vernalization response element), which is involved in responsiveness to cold treatment (30, 31). Expression of *FLC* has been reported to be repressed by long-term cold treatment (vernalization), accompanied by enrichment of tri-methylation of histone H3 lysine 27 (H3K27me3) at the TSS site in the beginning of cold treatment, and then by H3K27me3 accumulation across gene body region after the plants returned to warmer temperatures (32). On the contrary, the expression of genes is associated with the removal of H3K27me3 from their bodies (33). These reports and our results suggest that epigenetic regulation of *AhgFLC* gene might be responsible for seasonal removal of CHH methylation in its intronic repeat. The disruption of transcription in genes has been reported to induce ectopic CHH methylation in *A. thaliana* (34).

Large-scale patterns of DNA methylation were constant throughout the year for all three contexts, although there were seasonal changes in DNA

bioRxiv preprint doi: https://doi.org/10.1101/589465; this version posted March 29, 2019. The copyright holder for this preprint (which was not certified by peer review) is the author/funder, who has granted bioRxiv a license to display the preprint in perpetuity. It is made available under aCC-BY-NC-ND 4.0 International license.

235 methylation at some cytosine sites. Constant levels of CG methylation were
236 observed in gene body, and, furthermore, we found that genes with high levels of
237 gbM showed seasonal stability in their gene expression. Although the function of
238 gbM is still unclear (35), our results support previous reports, in *A. thaliana*, that
239 gbM associates with genes modestly expressed among different tissues and
240 experimental conditions (6, 36-38), and imply the importance of gbM under
241 seasonal environment in a natural habitat.

242 Currently, we cannot entirely explain the patterns of DNA methylation in
243 SeMCs, particularly in CG or CHG contexts. It is very likely that there are
244 unidentified processes associated with environmental responses of DNA
245 methylation that have not been studied under laboratory conditions. As
246 mentioned above, the question remains of how the epigenetic variations in
247 plants have been established in natural fluctuating environment (39, 40). Here,
248 we focused on representative environmental effects on DNA methylation in a
249 single clonal individual. In future studies of DNA methylation, we need to
250 evaluate not only genotype effects, but also, so called 'linage effects' that

bioRxiv preprint doi: https://doi.org/10.1101/589465; this version posted March 29, 2019. The copyright holder for this preprint (which was not certified by peer review) is the author/funder, who has granted bioRxiv a license to display the preprint in perpetuity. It is made available under aCC-BY-NC-ND 4.0 International license.

represent past genetic and environmental effects. Furthermore, we should test to what extent seasonal changes in DNA methylation contribute to the variation in phenotypes in natural environments.

Materials and Methods

Plant materials. This study was conducted in a natural population of *Arabidopsis halleri* subsp. *gemmifera* located in central Japan (Omoide-gawa site, Naka-ku, Taka-cho, Hyogo Pref., 35°06' N, 134°55' E, altitude 190–230 m). Details of the study site have been described previously (19, 20). Leaf samples were collected at noon on the following dates: November 11 and December 22, 2014, and February 9, March 24, May 7, June 23, July 28, and September 8, 2015. In the study site, *A. halleri* forms patches of rosettes that consist of clonally propagated plants and sometimes genetically-related seed-originated plants. Originally six small patches of plants were chosen for leaf sampling, three of them were used for further analyses because the others were heavily damaged by deer herbivory between November 11 and December 22 in 2014. At each

bioRxiv preprint doi: https://doi.org/10.1101/589465; this version posted March 29, 2019. The copyright holder for this preprint (which was not certified by peer review) is the author/funder, who has granted bioRxiv a license to display the preprint in perpetuity. It is made available under aCC-BY-NC-ND 4.0 International license.

sampling date, we harvested multiple mature and intact leaves from each plant. Each leaf was ca. 3-cm long, and weighed ca. 0.1 g. To detect DNA methylation and RNA expression in the same set of leaves, a small piece was collected from each leaf for RNA extraction. For DNA extraction, leaves were frozen in an ethanol bath with dry ice, then stored at -80 °C. For RNA extraction, the small pieces of leaves were stored in RNA*later* solution (Invitrogen, Carlsbad, CA, USA), then stored at -20 °C according to the manufacturer's instructions. The data for one patch were analyzed and shown in the main text, because the other two patches were found to be genetically mixed (Fig. S5). The samples analyzed here were confirmed to share whole-genome SNPs at levels that were safely judged to be a single clone (Fig. S5).

DNA extraction and WGBS library preparation. Genomic DNA was extracted from collected leaves (two leaves per plant, ca. 0.2 g) using the CTAB method (41). Libraries for WGBS were constructed as described previously (42). Sequencing was performed with the Illumina Hiseq 2500 system.

bioRxiv preprint doi: https://doi.org/10.1101/589465; this version posted March 29, 2019. The copyright holder for this preprint (which was not certified by peer review) is the author/funder, who has granted bioRxiv a license to display the preprint in perpetuity. It is made available under aCC-BY-NC-ND 4.0 International license.

283

284 **Processing of WGBS data.** Sequenced reads were trimmed using
285 Trimmomatic (43). Trimmed reads were mapped onto the genome sequence of
286 *A. halleri* (44) using Bismark (45) and Bowtie2 (46). Repetitive sequences in the
287 genome were detected using RepeatModeler (47), and repeats with at least 50
288 bp length were used for further analyses. The level of DNA methylation was
289 calculated for each context using the ratio of the number of methylated cytosines
290 to the number of total sequenced cytosine included in any region of the genome.
291 Efficient bisulfite treatment (> 99% in all samples) was confirmed using the level
292 of DNA methylation in unmethylated lambda DNA (Table S4). SeMC was defined
293 as any cytosine differently methylated between at least two time points, detected
294 by Fisher's exact test, with genome-wide FDRs that were calculated using
295 Storey's method (48). To draw the heatmaps of methylation of SeMCs, cluster
296 3.0 (49) and Java Treeview (50) were used. To draw a circos plot for
297 scaffold-wide DNA methylation, Circos software (51) was used. To make
298 browser views of DNA methylation, Integrated Genome Viewer (52) was used.

bioRxiv preprint doi: https://doi.org/10.1101/589465; this version posted March 29, 2019. The copyright holder for this preprint (which was not certified by peer review) is the author/funder, who has granted bioRxiv a license to display the preprint in perpetuity. It is made available under aCC-BY-NC-ND 4.0 International license.

299 To draw a dendrogram of collected samples, MethylExtract (53), VCF-kit
300 (https://vcf-kit.readthedocs.io), and Dendroscope3 (54) were used.
301
302 **Transcriptome analysis.** RNA extraction and library preparation for RNA-seq
303 were performed using the shotgun type method of BrAD-seq protocol (55).
304 Sequencing was performed with the Illumina Hiseq 2500 system. Mapping of the
305 reads and calculation of RPM were processed as described previously (21)
306 except that the reference sequence was replaced with a newer annotation (44).
307 To calculate seasonal average and range of expression of genes more precisely,
308 weekly sampled RNA-seq data from a two-year period (21) were re-analyzed. To
309 quantify the expression, Kallisto software was used (56). Calculation of seasonal
310 average and range of RNA expression was based on previously described
311 methods (21).
312
313 **Data availability**
314 Raw WGBS and RNA-Seq reads are available under the DDBJ BioProject

bioRxiv preprint doi: https://doi.org/10.1101/589465; this version posted March 29, 2019. The copyright holder for this preprint (which was not certified by peer review) is the author/funder, who has granted bioRxiv a license to display the preprint in perpetuity. It is made available under aCC-BY-NC-ND 4.0 International license.

315 PRJDB7785.

316

317 **Acknowledgement**

318 We thank Jiro Sugisaka for technical assistance, Takaomi Hatakeyama for
319 information on *A. halleri* genome sequence, Atsushi J. Nagano for advice on
320 analysis of RNA-seq data, and Kentaro K. Shimizu for comments on the
321 manuscript. Computations were partially performed on the NIG supercomputer
322 at NIG, Japan. This study was supported by JSPS Grant-in-Aid for Scientific
323 Research (S) 26221106 and JST CREST JPMJCR15O1 to HK; Grant-in-Aid for
324 JSPS Fellows by Japanese Society for Promoting Science (17J02659) to TI;
325 Systems Functional Genetics Project of the Transdisciplinary Research
326 Integration Center, ROIS, Japan to A.T., A.F., Y.T., and T.K.

327

328 **Author contributions**

329 H.K. and T.K. conceived the study. T.I., H.N., H.K., and T.K. designed the
330 experiments. H.N. collected samples. Y.T., A.T., and A.F. performed

bioRxiv preprint doi: https://doi.org/10.1101/589465; this version posted March 29, 2019. The copyright holder for this preprint (which was not certified by peer review) is the author/funder, who has granted bioRxiv a license to display the preprint in perpetuity. It is made available under aCC-BY-NC-ND 4.0 International license.

331 whole-genome bisulfite sequencing. N.E. and M.N.H. performed RNA
332 sequencing. T.I. analyzed the data. T.I. and H.K. wrote the paper and
333 incorporated comments from co-authors.

334

335 **Conflict of interest**

336 The authors declare that they have no conflicts of interests.

337

338 **References**

339 1. Law JA, Jacobsen SE (2010) Establishing, maintaining and modifying DNA
340 methylation patterns in plants and animals. *Nat Rev Genet* 11:204–220.
341 2. Cokus SJ, et al. (2008) Shotgun bisulphite sequencing of the *Arabidopsis*
342 genome reveals DNA methylation patterning. *Nature* 452:215–219.
343 3. Lister R, et al. (2008) Highly integrated single-base resolution maps of the
344 epigenome in *Arabidopsis*. *Cell* 133:523–536.
345 4. Lister R, et al. (2009) Human DNA methylomes at base resolution show
346 widespread epigenomic differences. *Nature* 462:315–322.

bioRxiv preprint doi: https://doi.org/10.1101/589465; this version posted March 29, 2019. The copyright holder for this preprint (which was not certified by peer review) is the author/funder, who has granted bioRxiv a license to display the preprint in perpetuity. It is made available under aCC-BY-NC-ND 4.0 International license.

5. Feng S, et al. (2010) Conservation and divergence of methylation patterning in plants and animals. *Proc Natl Acad Sci USA* 107:8689–8694.

6. Zemach A, McDaniel IE, Silva P, Zilberman D (2010) Genome-wide evolutionary analysis of eukaryotic DNA methylation. *Science* 328:916–919.

7. Huff JT, Zilberman D (2014) Dnmt1-Independent CG methylation contributes to nucleosome positioning in diverse eukaryotes. *Cell* 156:1286–1297.

8. Niederhuth CE, et al. (2016) Widespread natural variation of DNA methylation within angiosperms. *Genome Biol* 17:194.

9. Cubas P, Vincent C, Coen E (1999) An epigenetic mutation responsible for natural variation in floral symmetry. *Nature* 401:157–161.

10. Manning K, et al. (2006) A naturally occurring epigenetic mutation in a gene encoding an SBP-box transcription factor inhibits tomato fruit ripening. *Nat Genet* 38:948–952.

11. Ong-Abdullah M, et al. (2015) Loss of Karma transposon methylation underlies the mantled somaclonal variant of oil palm. *Nature* 525:533–537.

12. Dowen RH, et al. (2012) Widespread dynamic DNA methylation in response

bioRxiv preprint doi: https://doi.org/10.1101/589465; this version posted March 29, 2019. The copyright holder for this preprint (which was not certified by peer review) is the author/funder, who has granted bioRxiv a license to display the preprint in perpetuity. It is made available under aCC-BY-NC-ND 4.0 International license.

363 to biotic stress. *Proc Natl Acad Sci USA* 109:E2183–E2191.

364 13. Dubin MJ, et al. (2015) DNA methylation in *Arabidopsis* has a genetic basis

365 and shows evidence of local adaptation. *eLife* 4:elife.05255.

366 14. Secco D, et al. (2015) Stress induced gene expression drives transient DNA

367 methylation changes at adjacent repetitive elements. *eLife* 4:e09343.

368 15. Becker C, et al. (2011) Spontaneous epigenetic variation in the *Arabidopsis*

369 *thaliana* methylome. *Nature* 480:245–249.

370 16. Schmitz RJ, et al. (2011) Transgenerational epigenetic instability is a source

371 of novel methylation variants. *Science* 334:369–373.

372 17. Shimizu KK, Kudoh H, Kobayashi MJ (2011) Plant sexual reproduction

373 during climate change: gene function *in natura* studied by ecological and

374 evolutionary systems biology. *Ann Bot* 108:777–787.

375 18. Kudoh H (2016) Molecular phenology in plants: *in natura* systems biology for

376 the comprehensive understanding of seasonal responses under natural

377 environments. *New Phytol* 210:399–412.

378 19. Kudoh H, Honjo MN, Nishio H, Sugisaka J (2018) The long-term "*in natura*"

bioRxiv preprint doi: https://doi.org/10.1101/589465; this version posted March 29, 2019. The copyright holder for this preprint (which was not certified by peer review) is the author/funder, who has granted bioRxiv a license to display the preprint in perpetuity. It is made available under aCC-BY-NC-ND 4.0 International license.

379 study sites of *Arabidopsis halleri* for plant transcription and epigenetic
380 modification analyses in natural environments. *Methods Mol Biol* 1830:41–
381 57.

382 20. Aikawa S, Kobayashi MJ, Satake A, Shimizu KK, Kudoh H (2010) Robust
383 control of the seasonal expression of the Arabidopsis *FLC* gene in a
384 fluctuating environment. *Proc Natl Acad Sci USA* 107:11632–11637.

385 21. Nagano AJ, et al. (2019) Annual transcriptome dynamics in natural
386 environments reveals plant seasonal adaptation. *Nat Plants* 5:74–83.

387 22. Stroud H, et al. (2013) Non-CG methylation patterns shape the epigenetic
388 landscape in *Arabidopsis*. *Nat Struct Mol Biol* 21:64–72.

389 23. Kawashima T, Berger F (2014) Epigenetic reprogramming in plant sexual
390 reproduction. *Nat Rev Genet* 15:613–624.

391 24. He Y, Ecker JR (2015) Non-CG methylation in the human genome. *Annu Rev*
392 *Genomics Hum Genet* 16:55–77.

393 25. Seymour DK, Koenig D, Hagmann J, Becker C, Weigel D (2014) Evolution of
394 DNA methylation patterns in the Brassicaceae is driven by differences in

bioRxiv preprint doi: https://doi.org/10.1101/589465; this version posted March 29, 2019. The copyright holder for this preprint (which was not certified by peer review) is the author/funder, who has granted bioRxiv a license to display the preprint in perpetuity. It is made available under aCC-BY-NC-ND 4.0 International license.

genome organization. *PLoS Genet* 10:e1004785.

26. Fedoroff NV (2012) Transposable elements, epigenetics, and genome evolution. *Science* 338:758–767.

27. Tenaillon MI, Hollister JD, Gaut BS (2010) A triptych of the evolution of plant transposable elements. *Trends Plant Sci* 15:471–478.

28. Czechowski T (2005) Genome-wide identification and testing of superior reference genes for transcript normalization in Arabidopsis. *Plant Physiol* 139:5–17.

29. Popova OV, Dinh HQ, Aufsatz W, Jonak C (2013) The RdDM Pathway Is required for basal heat tolerance in *Arabidopsis*. *Mol Plant* 6:396–410.

30. Sung S, et al. (2006) Epigenetic maintenance of the vernalized state in *Arabidopsis thaliana* requires LIKE HETEROCHROMATIN PROTEIN 1. *Nat Genet* 38:706–710.

31. Castaings L, et al. (2014) Evolutionary conservation of cold-induced antisense RNAs of *FLOWERING LOCUS C* in *Arabidopsis thaliana* perennial relatives. *Nat Commun* 5:4457. doi:10.1038/ncomms5457.

bioRxiv preprint doi: https://doi.org/10.1101/589465; this version posted March 29, 2019. The copyright holder for this preprint (which was not certified by peer review) is the author/funder, who has granted bioRxiv a license to display the preprint in perpetuity. It is made available under aCC-BY-NC-ND 4.0 International license.

411 32. Song J, Irwin J, Dean C (2013) Remembering the prolonged cold of winter.
412 *Curr Biol* 23:R807–R811.
413 33. Buzas DM, Robertson M, Finnegan EJ, Helliwell CA (2011)
414 Transcription-dependence of histone H3 lysine 27 trimethylation at the
415 Arabidopsis polycomb target gene *FLC*. *Plant J* 65:872–881.
416 34. Inagaki S, et al. (2010) Autocatalytic differentiation of epigenetic
417 modifications within the Arabidopsis genome. *EMBO J* 29:3496–3506.
418 35. Zilberman D (2017) An evolutionary case for functional gene body
419 methylation in plants and animals. *Genome Biol* 18:87.
420 36. Zhang X, et al. (2006) Genome-wide high-resolution mapping and functional
421 analysis of DNA methylation in *Arabidopsis*. *Cell* 126:1189–1201.
422 37. Aceituno FF, Moseyko N, Rhee SY, Gutiérrez RA (2008) The rules of gene
423 expression in plants: Organ identity and gene body methylation are key
424 factors for regulation of gene expression in *Arabidopsis thaliana*. *BMC*
425 *Genomics* 9:438.
426 38. Coleman-Derr D, Zilberman D (2012) Deposition of histone variant H2A.Z

bioRxiv preprint doi: https://doi.org/10.1101/589465; this version posted March 29, 2019. The copyright holder for this preprint (which was not certified by peer review) is the author/funder, who has granted bioRxiv a license to display the preprint in perpetuity. It is made available under aCC-BY-NC-ND 4.0 International license.

within gene bodies regulates responsive genes. *PLoS Genet* 8:e1002988.

39. Richards EJ (2006) Inherited epigenetic variation — revisiting soft inheritance. *Nat Rev Genet* 7:395–401.

40. Weigel D, Colot V (2012) Epialleles in plant evolution. *Genome Biol* 13:249.

41. Saghai-Maroof MA, Soliman KM, Jorgensen RA, Allard RW (1984) Ribosomal DNA spacer-length polymorphisms in barley: mendelian inheritance, chromosomal location, and population dynamics. *Proc Natl Acad Sci USA* 81:8014–8018.

42. Fu Y, et al. (2013) Mobilization of a plant transposon by expression of the transposon-encoded anti-silencing factor. *EMBO J* 32:2407–2417.

43. Bolger AM, Lohse M, Usadel B (2014) Trimmomatic: a flexible trimmer for Illumina sequence data. *Bioinformatics* 30:2114–2120.

44. Briskine RV, et al. (2016) Genome assembly and annotation of *Arabidopsis halleri*, a model for heavy metal hyperaccumulation and evolutionary ecology. *Mol Ecol Resour* 17:1025–1036.

45. Krueger F, Andrews SR (2011) Bismark: a flexible aligner and methylation

bioRxiv preprint doi: https://doi.org/10.1101/589465; this version posted March 29, 2019. The copyright holder for this preprint (which was not certified by peer review) is the author/funder, who has granted bioRxiv a license to display the preprint in perpetuity. It is made available under aCC-BY-NC-ND 4.0 International license.

443 caller for Bisulfite-Seq applications. *Bioinformatics* 27:1571–1572.

444 46. Langmead B, Salzberg SL (2012) Fast gapped-read alignment with Bowtie 2.

445 *Nat Methods* 9:357–359.

446 47. Smit AFA, Hubley R (2008-2015) RepeatModeler Open-1.0.

447 http://www.repeatmasker.org.

448 48. Storey JD (2002) A direct approach to false discovery rates. *J R Stat Soc*

449 *Series B Stat Methodol* 64:479–498.

450 49. de Hoon MJL, Imoto S, Nolan J, Miyano S (2004) Open source clustering

451 software. *Bioinformatics* 20:1453–1454.

452 50. Saldanha AJ (2004) Java Treeview—extensible visualization of microarray

453 data. *Bioinformatics* 20:3246–3248.

454 51. Krzywinski M, et al. (2009) Circos: An information aesthetic for comparative

455 genomics. *Genome Res* 19:1639–1645.

456 52. Robinson JT, et al. (2011) Integrative genomics viewer. *Nat Biotechnol*

457 29:24–26.

458 53. Barturen G, Rueda A, Oliver JL, Hackenberg M (2013) Methylextract.

bioRxiv preprint doi: https://doi.org/10.1101/589465; this version posted March 29, 2019. The copyright holder for this preprint (which was not certified by peer review) is the author/funder, who has granted bioRxiv a license to display the preprint in perpetuity. It is made available under aCC-BY-NC-ND 4.0 International license.

459 doi:10.5281/zenodo.7144.

460 54. Huson DH, Scornavacca C (2012) Dendroscope 3: An Interactive Tool for

461 Rooted Phylogenetic Trees and Networks. *Syst Biol* 61:1061–1067.

462 55. Townsley BT, Covington MF, Ichihashi Y, Zumstein K, Sinha NR (2015)

463 BrAD-seq: Breath Adapter Directional sequencing: a streamlined,

464 ultra-simple and fast library preparation protocol for strand specific mRNA

465 library construction. *Front Plant Sci* 6. doi:10.3389/fpls.2015.00366.

466 56. Bray NL, Pimentel H, Melsted P, Pachter L (2016) Near-optimal probabilistic

467 RNA-seq quantification. *Nat Biotechnol* 34:525–527.

bioRxiv preprint doi: https://doi.org/10.1101/589465; this version posted March 29, 2019. The copyright holder for this preprint (which was not certified by peer review) is the author/funder, who has granted bioRxiv a license to display the preprint in perpetuity. It is made available under aCC-BY-NC-ND 4.0 International license.

468 **Figure Legends**

469

470 **Fig. 1.** Sampling site and dates for the seasonal DNA-methylation analysis in a
471 natural population of *Arabidopsis halleri* subsp. *gemmifera*. (*A*) A photograph of
472 the study site alongside a small stream through the *Cryptomeria* and
473 *Chamaecyparis* plantation in Hyogo Prefecture, Japan. Red arrows indicate
474 individuals of *A. halleri.* (*B*) An individual of *A. halleri* in the study site. The cage
475 was used for protection against deer herbivory. White bar indicates 100 mm. (*C*)
476 Sampling dates (8 time points) and temperature regimes during the study period.
477 Sampling was performed every ca. 1.5 month for a year. The red line indicates
478 hourly air temperature, and dotted lines represent timings of the sampling.

479

480 **Fig. 2.** Genomic pattern of DNA methylation across a year. (*A*) A circos plot
481 showing seasonal patterns (8 time points) of DNA methylation in CG, CHG, and
482 CHH contexts for the longest 30 scaffolds of *A. hallleri.* On the outermost circle,
483 scaffold positions are indicated by numbers and black bars with scales (one

bioRxiv preprint doi: https://doi.org/10.1101/589465; this version posted March 29, 2019. The copyright holder for this preprint (which was not certified by peer review) is the author/funder, who has granted bioRxiv a license to display the preprint in perpetuity. It is made available under aCC-BY-NC-ND 4.0 International license.

484 scale = 0.4 Mbp). Each shaded/colored circle represents the scaffold-wide
485 distribution of genomic attributes for each 100-Kb window. The second
486 outermost circle represents density of repetitive sequences (including
487 transposable elements). Each tile indicates the density: the lowest in white, the
488 highest in black (0–0.5). The next 24 circles represent DNA methylation levels at
489 8 time points (starting from Nov 24, 2014 to Sep 8, 2015, towards the inner
490 circles shown by the arrows) for CG, CHG, and CHH contexts, respectively.
491 Colors in each tile indicates level of methylation: the lowest as blue, the highest
492 as red (0–0.9 for CG context, 0–0.5 for the others). (*B*) Scattering plots
493 comparing CG, CHG, and CHH DNA methylation against TE density for all 100
494 kbp windows across the 30 scaffolds.
495
496 **Fig. 3.** Annual patterns of seasonally-methylated cytosines (SeMCs). (*A*)
497 Heatmaps of seasonally methylated cytosines (SeMCs) in CG, CHG, and CHH
498 contexts (from left to right; n = 62,716, 47,140, 179,385, respectively). Each row
499 indicates a series of DNA methylation ratios across a year in each position in the

bioRxiv preprint doi: https://doi.org/10.1101/589465; this version posted March 29, 2019. The copyright holder for this preprint (which was not certified by peer review) is the author/funder, who has granted bioRxiv a license to display the preprint in perpetuity. It is made available under aCC-BY-NC-ND 4.0 International license.

genome (0: unmethylated, 1; fully methylated). The dendrogram on the left of each heatmap represents the result of hierarchical clustering of SeMCs. Distance in the dendrogram was based on Pearson's correlation coefficient. (*B*) Barplot showing the distribution of peak timings of methylation level for the SeMCs in CG, CHG, and CHH contexts (from left to right, respectively).

Fig. 4. SeMCs in the CG, CHG, and CHH contexts, and seasonal patterns in CHH DNA methylation levels. (*A*) Pie charts indicating locations (exon, intron, and intergenic regions) of seasonally methylated cytosines (SeMCs) in CG, CHG, and CHH contexts (from left to right, respectively). (*B*) Boxplots of CHH methylation at 8 time points in repetitive elements. The boxes span from the first to the third quartiles, the thick black bars inside the boxes are the medians, whiskers above and below the boxes represent 1.5 × interquartile ranges from the quartiles. Dotted line indicates the median CHH methylation level in Nov. 2014. (*C* and *D*) Browser views for seasonal patterns of CHH methylation on repeat sequences in one of LINE/L1 sequences (*C*) and *AhgFLC* locus (*D*).

bioRxiv preprint doi: https://doi.org/10.1101/589465; this version posted March 29, 2019. The copyright holder for this preprint (which was not certified by peer review) is the author/funder, who has granted bioRxiv a license to display the preprint in perpetuity. It is made available under aCC-BY-NC-ND 4.0 International license.

516 Orange rectangles indicates exons. A gray rectangle in the *AhgFLC* locus
517 indicates a repetitive sequence. (*E*) Comparison between RNA expression of
518 *AhgFLC* and CHH methylation of the repetitive sequence in its intron.
519
520 **Fig. 5. CG DNA methylation and stability of gene expression.** (*A*-*D*) Browser
521 views of seasonal patterns of CG methylation (*A* and *C*) and the two-year
522 dynamics of RNA expression level (*B* and *D*; from September 2011 to August
523 2013) for *AhgPP2AA3* (*g04731*) and *AhgFLC* (*g19190*), respectively. Orange
524 rectangles indicate exons. A gray rectangle indicates a repetitive sequence in
525 the *AhgFLC* locus. (E, F) Boxplots showing relationship between DNA
526 methylation in CG context and the average (E) and range (F) of RNA expression
527 of genes. Only expressed genes (average expression level (log2(RPM) > 1)) are
528 used for these analyses. Genes were split into five bins according to quintiles of
529 genic DNA methylation in CG context. The boxes span from the first to the third
530 quartiles, the bands inside the boxes are the medians, whiskers above and
531 below the boxes represent 1.5 × interquartile ranges from the quartiles. Different

bioRxiv preprint doi: https://doi.org/10.1101/589465; this version posted March 29, 2019. The copyright holder for this preprint (which was not certified by peer review) is the author/funder, who has granted bioRxiv a license to display the preprint in perpetuity. It is made available under aCC-BY-NC-ND 4.0 International license.

letters represent significant differences between groups in the Mann-Whitney test, $P < 0.01$ adjusted for multiple comparisons.

Fig. S1. Genome-wide bulk DNA methylation level at eight time points across a year. Genome-wide bulk DNA methylation levels are shown in CG, CHG, and CHH context for the whole genome (*A*), and gene and repetitive sequences (*B*). Eight sampling timings are represented by the different shades.

Fig. S2. DNA methylation was seasonally stable at a majority of CG, CHG, and CHH sites. Histograms of seasonal differences of DNA methylation (max. – min.) for all cytosine sites (*A*), and for SeMCs (*B*) in CG, CHG, and CHH contexts.

Fig. S3. Seasonal patterns in CHH DNA methylation in repetitive elements that belong to the six major families of transposable elements (TEs). The boxes span from the first to the third quartiles, the thick black bars inside the boxes are the medians, whiskers above and below the boxes represent 1.5 × interquartile

bioRxiv preprint doi: https://doi.org/10.1101/589465; this version posted March 29, 2019. The copyright holder for this preprint (which was not certified by peer review) is the author/funder, who has granted bioRxiv a license to display the preprint in perpetuity. It is made available under aCC-BY-NC-ND 4.0 International license.

548 ranges from the quartiles.

549

550 **Fig. S4.** Seasonal patterns in CG gene body methylation (gbM) across a year.
551 (*A*) Boxplot of DNA methylation in genes in CG context at eight time points
552 across a year. The boxes span from the first to the third quartiles, the thick black
553 bars inside the boxes are the medians, whiskers above and below the boxes
554 represent 1.5 × interquartile ranges from the quartiles. (*B*) A histogram of
555 seasonal difference for DNA methylation in genes (max. – min.) in CG context.

556

557 **Fig. S5.** Some patches of A. halleri turned to be genetically mixed. A
558 dendrogram shows Kimura's genetic distance using genome-wide SNPs among
559 the samples in three patches for eight timepoints. The samples from replicate 1
560 were judged to be a single clone. A. halleri is an obligate outcrossing species
561 with a self-incompatible breeding system, and therefore a large portion of SNPs
562 are expected to be heterozygous. Because heterozygous SNPs can be
563 designated as homozygous to either of the alleles in a certain probability, a
564 terminal radial branching is expected to be observed even for genetically
565 identical plants that belong to a single clonal patch (Rep. 1).

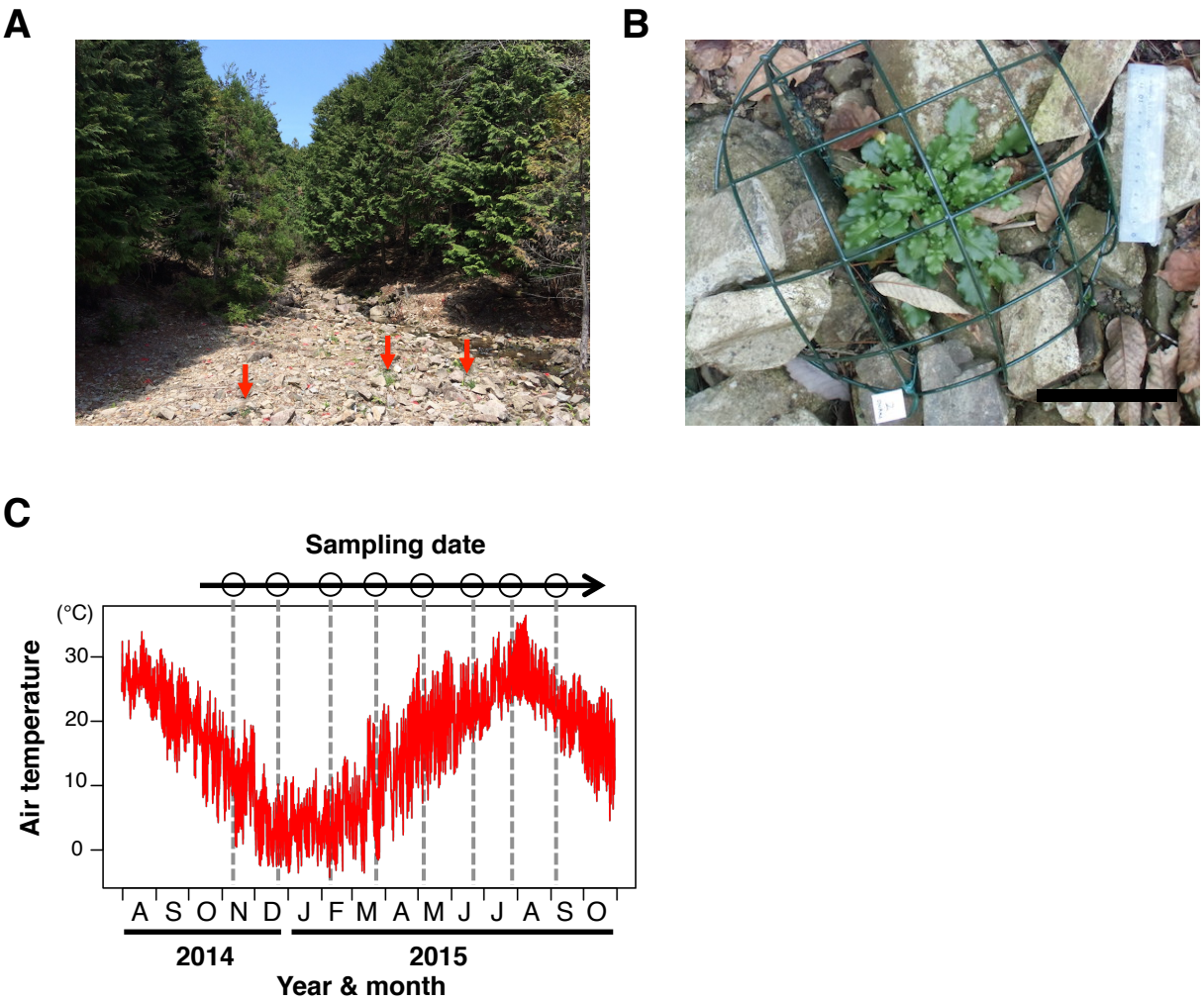

Fig. 1. Sampling site and dates for the seasonal DNA-methylation analysis in a natural population of *Arabidopsis halleri* subsp. *gemmifera*. (*A*) A photograph of the study site alongside a small stream through the *Cryptomeria* and *Chamaecyparis* plantation in Hyogo Prefecture, Japan. Red arrows indicate individuals of *A. halleri*. (*B*) An individual of *A. halleri* in the study site. The cage was used for protection against deer herbivory. White bar indicates 100 mm. (*C*) Sampling dates (8 time points) and temperature regimes during the study period. Sampling was performed every ca. 1.5 month for a year. The red line indicates hourly air temperature, and dotted lines represent timings of the sampling.

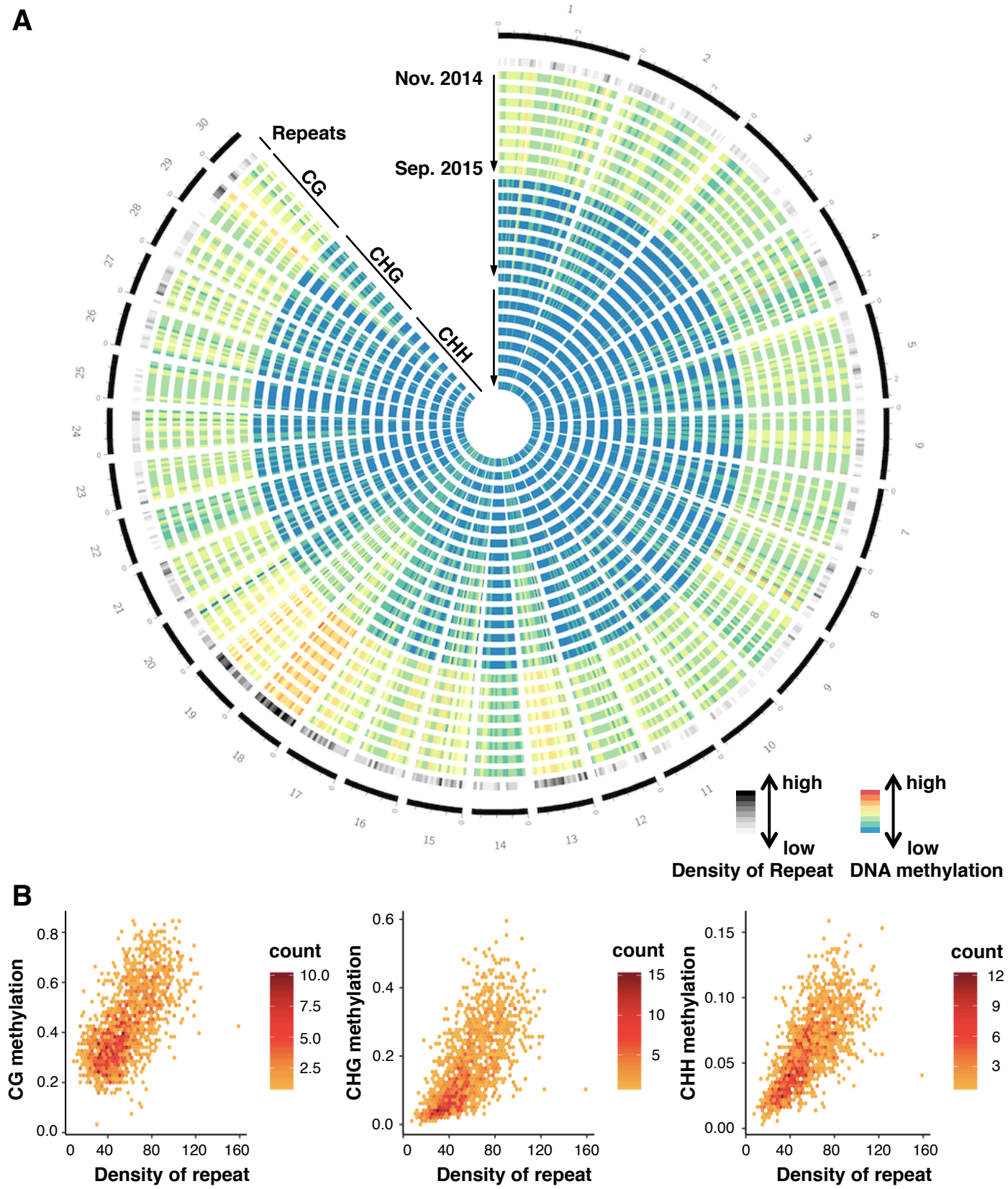

Fig. 2. Genomic pattern of DNA methylation across a year. (*A*) A circos plot showing seasonal patterns (8 time points) of DNA methylation in CG, CHG, and CHH contexts for the longest 30 scaffolds of *A. hallleri.* On the outermost circle, scaffold positions are indicated by numbers and black bars with scales (one scale = 0.4 Mbp). Each shaded/colored circle represents the scaffold-wide distribution of genomic attributes for each 100-Kb window. The second outermost circle represents density of repetitive sequences (including transposable elements). Each tile indicates the density: the lowest in white, the highest in black (0–0.5). The next 24 circles represent DNA methylation levels at 8 time points (starting from Nov 24, 2014 to Sep 8, 2015, towards the inner circles shown by the arrows) for CG, CHG, and CHH contexts, respectively. Colors in each tile indicates level of methylation: the lowest as blue, the highest as red (0–0.9 for CG context, 0–0.5 for the others). (*B*) Scattering plots comparing CG, CHG, and CHH DNA methylation against TE density for all 100 kbp windows across the 30 scaffolds.

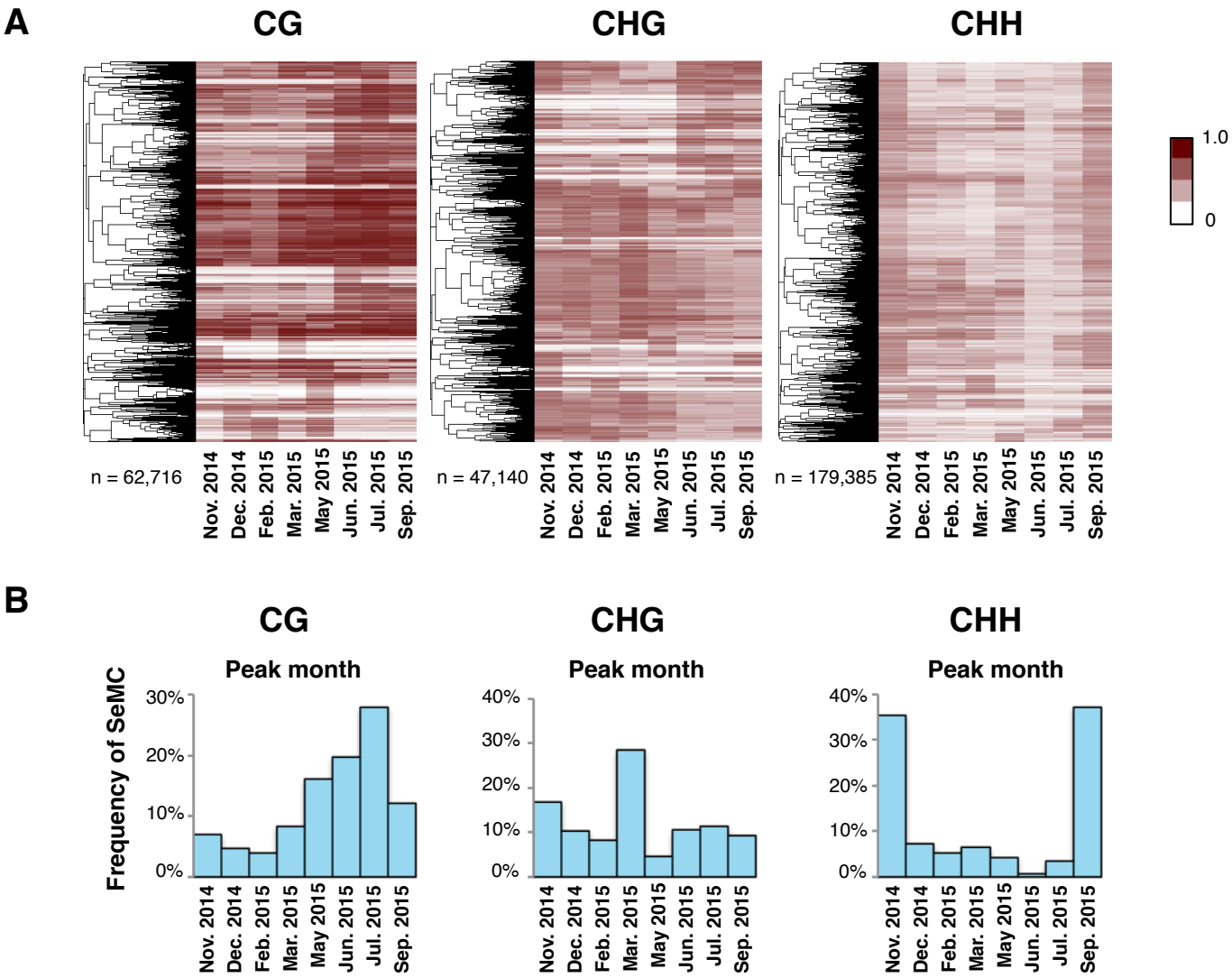

Fig. 3. Annual patterns of seasonally-methylated cytosines (SeMCs). (*A*) Heatmaps of seasonally methylated cytosines (SeMCs) in CG, CHG, and CHH contexts (from left to right; n = 62,716, 47,140, 179,385, respectively). Each row indicates a series of DNA methylation ratios across a year in each position in the genome (0: unmethylated, 1; fully methylated). The dendrogram on the left of each heatmap represents the result of hierarchical clustering of SeMCs. Distance in the dendrogram was based on Pearson's correlation coefficient. (*B*) Barplot showing the distribution of peak timings of methylation level for the SeMCs in CG, CHG, and CHH contexts (from left to right, respectively).

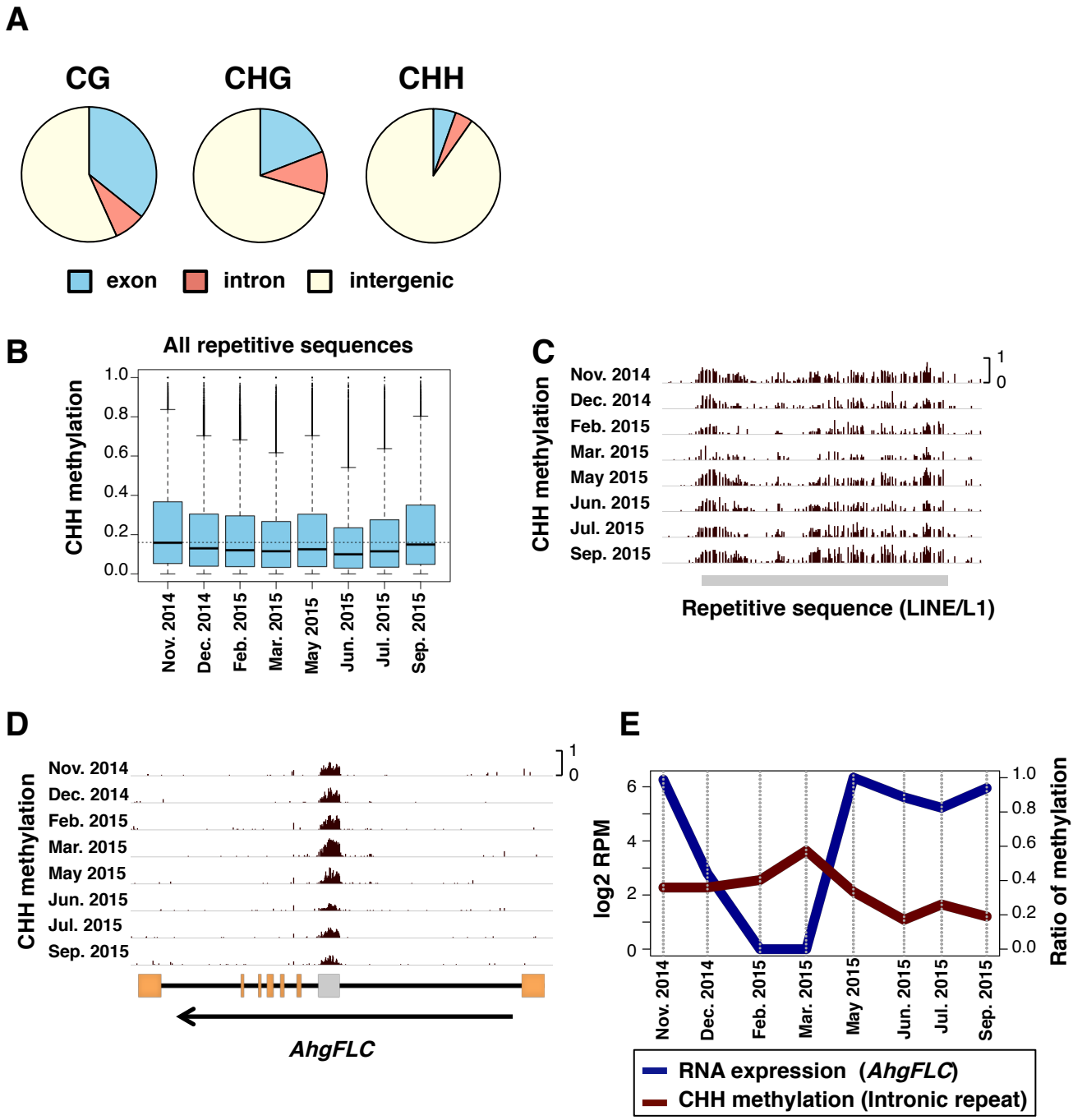

Fig. 4. SeMCs in the CG, CHG, and CHH contexts, and seasonal patterns in CHH DNA methylation levels. (*A*) Pie charts indicating locations (exon, intron, and intergenic regions) of seasonally methylated cytosines (SeMCs) in CG, CHG, and CHH contexts (from left to right, respectively). (*B*) Boxplots of CHH methylation at 8 time points in repetitive elements. The boxes span from the first to the third quartiles, the thick black bars inside the boxes are the medians, whiskers above and below the boxes represent 1.5 × interquartile ranges from the quartiles. Dotted line indicates the median CHH methylation level in Nov. 2014. (*C* and *D*) Browser views for seasonal patterns of CHH methylation on repeat sequences in one of LINE/L1 sequences (*C*) and *AhgFLC* locus (*D*). Orange rectangles indicates exons. A gray rectangle in the *AhgFLC* locus indicates a repetitive sequence. (*E*) Comparison between RNA expression of *AhgFLC* and CHH methylation of the repetitive sequence in its intron.

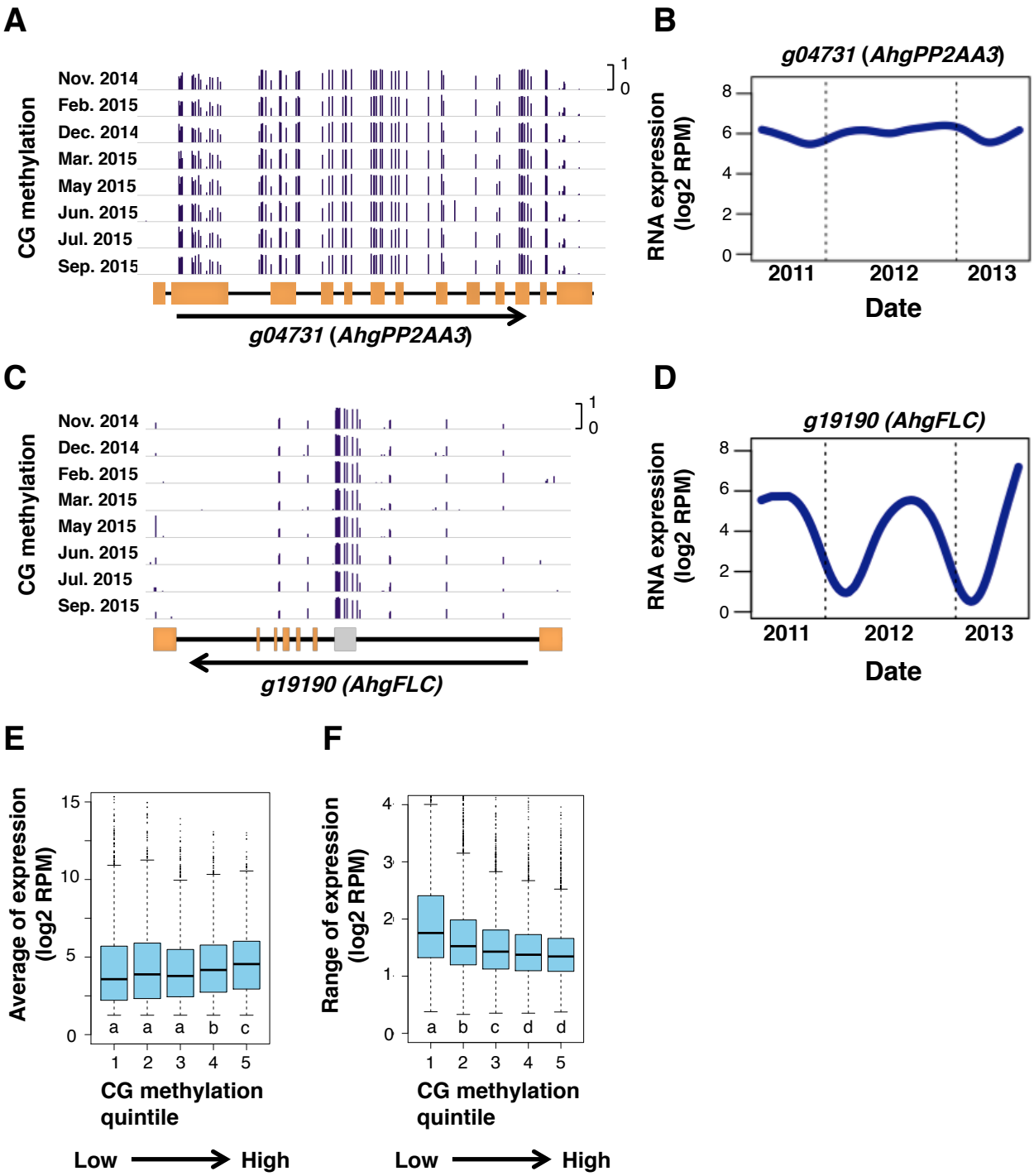

Fig. 5. CG DNA methylation and stability of gene expression. (*A-D*) Browser views of seasonal patterns of CG methylation (*A* and *C*) and the two-year dynamics of RNA expression level (*B* and *D*; from September 2011 to August 2013) for *AhgPP2AA3* (*g04731*) and *AhgFLC* (*g19190*), respectively. Orange rectangles indicate exons. A gray rectangle indicates a repetitive sequence in the *AhgFLC* locus. (E, F) Boxplots showing relationship between DNA methylation in CG context and the average (E) and range (F) of RNA expression of genes. Only expressed genes (average expression level (log2(RPM) > 1)) are used for these analyses. Genes were split into five bins according to quintiles of genic DNA methylation in CG context. The boxes span from the first to the third quartiles, the bands inside the boxes are the medians, whiskers above and below the boxes represent 1.5 × interquartile ranges from the quartiles. Different letters represent significant differences between groups in the Mann-Whitney test, $P < 0.01$ adjusted for multiple comparisons.